15TH IEA HEAT PUMP CONFERENCE
MAY 26–29, 2026 | HOFBURG
VIENNA 2026
DECARBONISATION THROUGH INNOVATION

Analysis on effect of cold air re-circulation on performance of heat collector units in Large-Scale Air-Source Heat Pumps (ASHPs)

Seyed Ehsan Rafiee[a*], Teemu Turunen-Saaresti[a], Antti Uusitalo[a], Valtteri Mikkola[b], Kari Jääskeläinen[b]

[a]LUT University, School of Energy Systems, Lappeenranta P. O. Box 20, 53851, Finland
[b]Fincoil LU-VE Oy, Vantaa 3 01740, Finland

Abstract

Large-scale air-source heat pumps (ASHPs) are increasingly recognized as essential technology for promoting sustainable heating and cooling solutions in urban and industrial settings. They provide an efficient and environmentally friendly alternative to traditional energy systems. This study presents a comprehensive three-dimensional computational fluid dynamics (3D-CFD) model designed to accurately capture the performance of heat collector of large-scale ASHPs under realistic environmental and operational conditions. Unlike previous models that often relied on simplified assumptions, this framework incorporates critical factors, such as, a: compressible flow, b: dynamic fan inlet and outlet temperatures, c: pressure variations along the fans, and d: variable mass flow rates influenced by fluctuations in air density. The model has been validated against experimental and numerical data from existing literature, demonstrating a strong agreement in volumetric effectiveness and flow characteristics. The results of this study provide valuable insights into the complex flow phenomena around the heat collector and their direct impact on the system performance. The impact of wind velocity (ranging from 0 *m/s* to 8 *m/s*) on the flow circulation around the device and the system's performance has been analyzed. As wind speed increases up to 5 *m/s*, efficiency declines due to enhanced vortex formation around the longer sides of the heat collector. This circulation of cold air to the inlets of the fans reduces system effectiveness. However, beyond this point, further increases in wind speed weaken these vortices, resulting in more stable airflow and improved system performance. Additionally, as the wind velocity increases from 0 to 8 *m/s*, it increasingly weakens the upstream vortex, resulting in improved working conditions for the fans located on the upstream side of the heat collector. These findings demonstrate a strong correlation between vortex behavior around the heat collectors and the overall operational efficiency of large-scale ASHPs.

Selection and/or peer-review under the responsibility of the organizers of the 15th IEA Heat Pump Conference 2026.

Keywords: Large-scale air source heat pump; recirculation rate; efficiency; wind velocity; heat collectors

1. Introduction

Global warming has become one of the most pressing challenges facing the world today, with rising greenhouse gas emissions contributing to climate change and environmental degradation [1]. Global temperatures are currently about 1.0 $°C$ higher than pre-industrial levels [2]. If carbon dioxide emissions continue at the current rate, this temperature increase is projected to exceed 1.5 $°C$ sometime between 2030 and 2052 [3]. Rising levels of atmospheric heat are mainly associated with the heavy reliance on fossil fuels for energy generation, heating, and cooling [4]. As the world shifts toward sustainable solutions, there is a growing focus on greener and more energy-efficient technologies. In this context, heat pump systems have gained prominence due to their ability to transfer heat rather than generate it directly. This approach leads to significant energy conservation and a reduced environmental impact [5]. Air-source heat pumps (ASHPs) are widely used

* Corresponding author. Tel.: +358442462333
E-mail address: seyedehsan.rafiee@lut.fi

15th IEA Heat Pump Conference 2026 - ICO7.1 - https://doi.org/10.23697/bhva-6c54

in both single-family and multi-family buildings due to their cost-effectiveness and ease of planning, installation, and maintenance. Their versatility and ability to operate efficiently in various climate conditions, along with their relative simplicity, make them an excellent choice among heating options ([6] and [7]). These systems can utilize ambient air as a heat source, even in low-temperature environments. Continuous technological innovations have significantly enhanced their performance and practicality, including the development of more efficient compressors, environmentally friendly refrigerants, and advanced control systems [8]. One major advantage of ASHPs is their scalability, making them suitable for various applications, from small systems to large district heating networks. Numerous studies have thoroughly investigated how ambient conditions affect the efficiency of small-scale air source heat pumps (ASHPs). These studies underline the significant influence of factors such as climate change ([9] and [10]), outdoor temperature ([11] and [12]), wind velocity ([13] and [14]), and humidity ([11], [15] and [16]) on their performance. Additionally, extensive analyses have been conducted on the effects of refrigerant specifications, including different types ([17] and [18]) and injection techniques [19]. Despite extensive research on small-scale systems, there is a significant gap in the literature regarding the performance, optimization, and operational challenges of large-scale ASHPs. Few studies have examined how ambient conditions specifically impact large-scale ASHPs, highlighting the need for further investigation in this area to enable their effective deployment on a larger scale. Rogié et al. [20] developed a three-dimensional (3D) computational fluid dynamics (CFD) model to analyze airflow and circulation patterns around a heat collector for a large-scale ASHP. Their study concluded that adjacent buildings increase turbulence levels, which in turn degrades the system's performance.

This significant research is one of the few published studies modeling heat collectors for large-scale air-source heat pumps (ASHPs) and makes a significant contribution to the field.

However, it incorporates certain simplifications that may affect the accuracy of the results. The model is based on the following assumptions: 1) the flow field is incompressible, 2) there is no pressure variation along the fans, 3) the temperature at the fan outlets is constant, and 4) the mass flow rate of the fans is fixed.

The present research introduces a sophisticated and comprehensive CFD model that addresses the limitations of previous studies and aims to provide a more accurate representation of real-world large-scale ASHP operations. The key innovations of this model include: 1) Treating airflow as compressible, which is essential for accurately simulating air behavior at larger scales; 2) Dynamically calculating the fan outlet temperature based on inlet conditions, allowing each fan to operate independently and closely following real operational scenarios; 3) Incorporating pressure changes along the fans to accurately account for energy variations; 4) Allowing the mass flow rate of fans to vary during simulations in response to changes in air density caused by temperature fluctuations at the inlet and outlet. Additionally, our model undergoes thorough validation against experimental and CFD data to establish its reliability. This validation ensures the accuracy of the simulated results, making the model a robust tool for detailed analysis. The novelty of our work lies in integrating all these advanced features into a single, coherent CFD framework that effectively captures the complexities of heat collector of large-scale ASHPs under various environmental conditions. This represents a significant advancement in understanding their detailed performance, particularly regarding the realistic effects of ambient factors and circulating conditions, which are crucial for optimizing design and operation in practical applications. This comprehensive approach provides valuable insights for researchers and industry stakeholders seeking to enhance the efficiency and deployment of large-scale ASHP systems.

2. Physical properties

The system being simulated in this research is one of the heat collector models developed and produced by Fincoil Lu-Ve Oy Company. All the structural parameters have been defined based on the real model. This system consists of 8 units, with each unit containing 14 individual fans organized in 7 rows, all rotating simultaneously at a speed of 500 *rpm* and positioned 4 meters above the ground (H_{FP}). To evaluate its performance, the system is divided into five distinct areas labeled from A1 to A5. The geometric parameters of the actual model are detailed in Table 1, which illustrates the placement and configuration of the fans within the units. The layout of the fans, the direction of the airflow, the areas affected, the naming convention for the fans, and the structural features of the system are illustrated in Figure 1.

Table 1 Geometrical parameters of the heat collector of the large-scale air source heat pump

Length (*mm*)	Fan	Height (*mm*)	Width (*mm*)	Intake Diameter (*mm*)	Fan centers (*mm*)	Units	Wind speed (*m/s*)	Wind Direction (*deg*)	Fan direction	Fan Inlet Air Velocity (*m/s*)
19600	112	4120	12800	1080	1800	8	0, 2, 5, 8	0	Up to Down	6.67

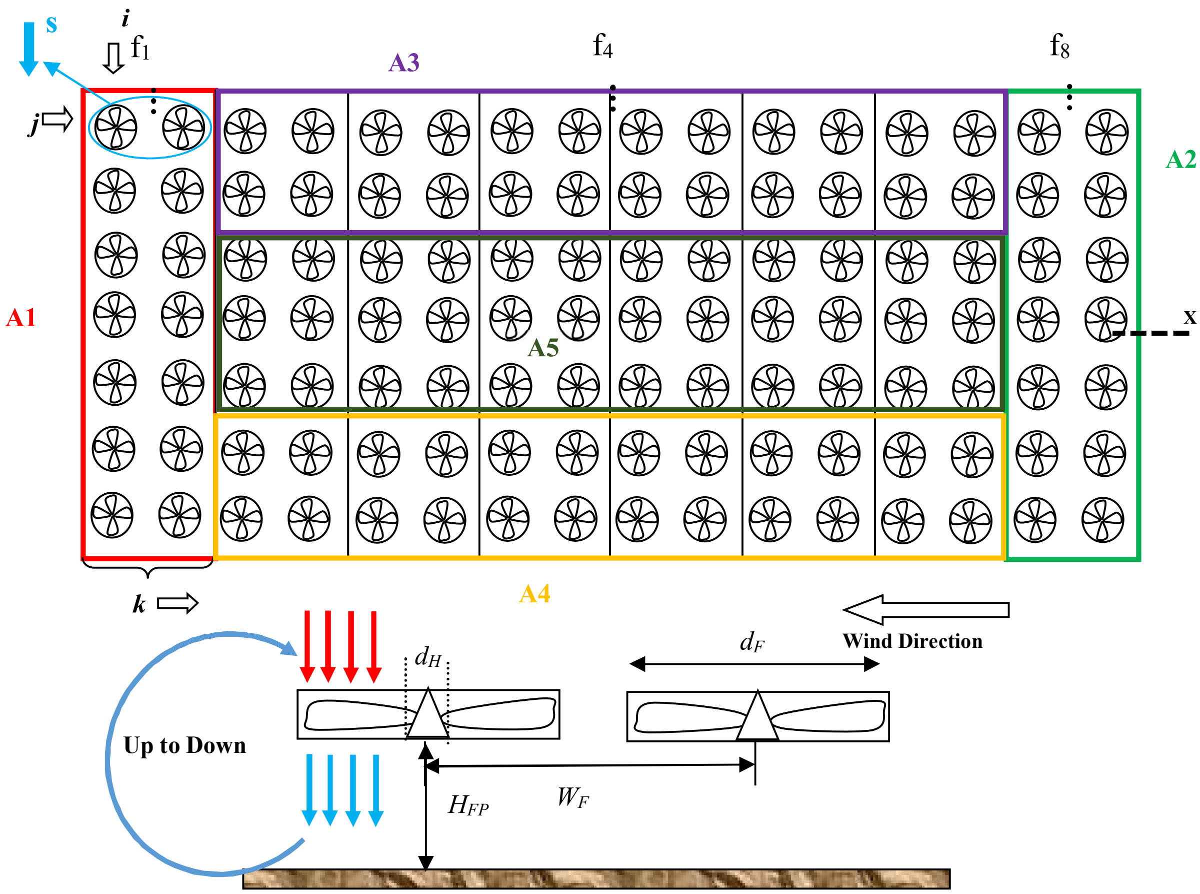

Figure 1 Schematic presentation of the considered heat collector of the large-scale air source heat pump with the related parameters

3. Computational details, domain structures and boundary conditions

The 3D-CFD model developed in this study was created in a simplified environment, free from obstacles such as nearby buildings. The turbulent flow field was simulated using the k-ε turbulence model in ANSYS Fluent 21R2 [21], which solves the continuity, momentum and energy equations using a density-based approach.

We used a second-order discretization scheme for the governing equations to enhance the accuracy of our numerical simulations. This approach allows for improved resolution of gradients and smoother variations in the flow field, which is essential for accurately capturing the complex behavior of airflow around the heat collector.

To ensure the reliability of our results, we set the residuals to a threshold of 10^{-8}. This indicates that the numerical solution achieved a sufficient level of convergence, meaning that changes in the solution between iterations were minimal. The convergence criteria were based on two key factors: the mass flow rate through the heat collector and the stability of the temperature within the computational domain.

By monitoring these parameters, we ensured that the simulation accurately represented the physical conditions of the system and that the results were both robust and reliable.

In this study, gravity is explicitly included as a key parameter in the simulations to accurately account for the effects of varying air density and buoyancy forces within the flow field. To ensure that the boundary conditions of the computational domain do not affect the thermophysical properties and behavior of the flow, the dimensions of the simulation domain (length, width, and height) are chosen to be twenty times larger than the size of the heat collector of the large-scale ASHP. This ample domain size helps minimize boundary effects, allowing the flow to develop naturally and closely resemble real-world conditions. By doing so, the simulation can better capture the complex interactions and performance characteristics of the flow, yielding results that are as representative and accurate as possible for practical applications.

The inlet of the computational domain is defined as a “Velocity Inlet” boundary condition, allowing the incoming airflow to be characterized by specific velocity parameters. The left, right, and top boundaries are set as "Symmetry" boundary conditions to reduce computational complexity while accurately representing the symmetry of the flow field. The bottom boundary is designated as a "Wall", with a "No-Slip boundary condition" applied to realistically simulate the effects of surface friction and the development of the boundary layer. The outlet of the domain is defined using a "Pressure Outlet" boundary condition, with ambient pressure specified to reflect typical atmospheric conditions, ensuring a natural flow exit from the simulation domain. Additionally, according to the assumptions provided by Fincoil Lu-Ve Oy, the outlet temperature of the fans is set to 0.4 times the inlet temperature. This reflects the typical thermal performance of the fan units under operational conditions.

This proportional relationship simplifies the modeling of heat transfer and fan behavior while maintaining a realistic representation of the system's thermal dynamics. Therefore, the input and output boundary conditions for each of the 112 fans are defined individually, as follows:

$$T_{Out}=0.4\ T_{in}\ (^oC) \tag{1}$$

Each fan operates independently, generating its own unique input and output data. During simulations, air density is dynamically updated at each calculation stage for both the inlet and outlet of all fans, resulting in a variable mass flow rate at the inlet. The boundary conditions at the fan inlet are defined based on a function of air density and volumetric flow rate, using a "mass flow inlet" boundary condition that takes these variables into account. Conversely, at the outlet of each fan, the mass flow rate is maintained equal to the inlet mass flow rate to ensure mass conservation.

This is achieved by defining the boundary condition as a "mass flow outlet," which corresponds to the calculated inlet flow. This approach enables a realistic simulation of the fans' behavior, effectively capturing the effects of changing density, temperature, and flow conditions throughout the system:

$$\dot{m}_{in}=Volumetric\ Flow\ Rate\ (m^3/s)\times Density\ (kg/m^3)\ and\ \dot{m}_{in}=\dot{m}_{out} \tag{2}$$

For each inlet, we have carefully considered the exact location of the electric motor that drives the fan to accurately represent the fan's geometry and flow characteristics. The entrances of the fans are designed with a donut-shaped (ring-shaped) profile, which mirrors the actual inlet configuration used in the physical system. To enhance both the accuracy and computational efficiency of the simulations, we employed a highly organized and structured grid throughout the entire computational domain (Figure 2).

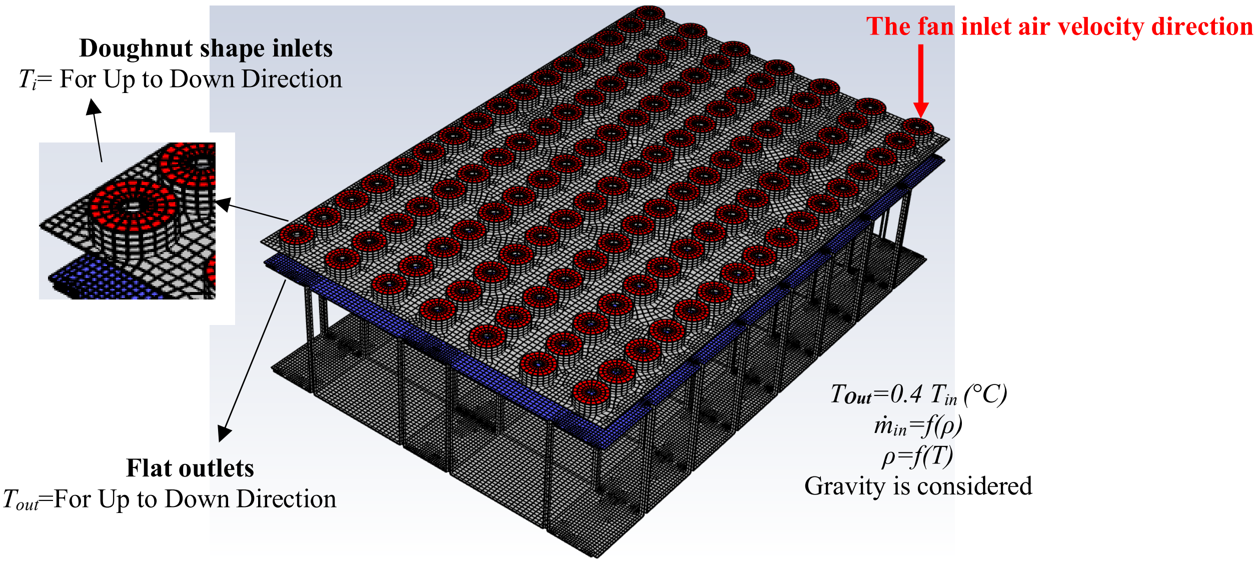

Figure 2 3D mesh grids, the shape and positions of inlets and outlets

This uniform grid arrangement provides finer resolution in critical areas, such as near the fan inlets and outlets, while still keeping the calculation times manageable. The shape and distribution of the grid elements, along with the detailed structure of the computational mesh, can be observed in the close-up view presented in Figure 2. This high-quality meshing approach allows us to accurately resolve flow features, minimizing numerical errors and ensuring reliable simulation results.

4. Grid independence study and validation

The total mass flow rate of the heat collector was used as the primary parameter for conducting the grid independence study. To ensure the reliability and accuracy of the CFD simulations, various mesh densities were tested to assess the impact of grid size on the results. As shown in Table 2, a comparison between the model using approximately 14.2 million grid cells and the one with around 17.5 million grid cells reveals a difference of only about 0.094% in the calculated mass flow rate. This minimal variation indicates that increasing the mesh density beyond 14.2 million cells yields negligible improvements in accuracy while significantly increasing computational costs. Therefore, we conclude that the model with 14.2 million mesh grids provides a sufficiently fine resolution to accurately capture the flow physics and can be confidently considered the baseline or reference model for subsequent analysis. This careful grid independence check ensures that the simulation results are both precise and stable, minimizing numerical errors associated with grid discretization.

Table 2 Results of grid independence study

Number of Grids (millions)	Total Mass Flow Rate (*kg/s*)
9.3	604.60
14.2	604.13 (the acceptable case)
17.5	604.07
21.1	604.05

This research utilizes the validation methodology proposed by Salta and Kröger [22]. In their laboratory study, they introduced the concept of volumetric effectiveness for fans, defined as the ratio of the actual volume flow rate passing through the fan (V) to the ideal, undisturbed flow volume (V_{id}). This effectiveness is expressed as a function of the vertical distance of the units from the ground, highlighting the impact of height and the surrounding environment on fan performance. By employing this validation approach, we can assess the accuracy of the CFD model based on how closely the simulated volumetric effectiveness aligns with the experimental data presented in their study:

$$V/V_{id}=0.985-exp^{-x} \tag{3}$$

Where:

$$X=\frac{(1+45/n_F)H_{FP}}{6.35d_F} \tag{4}$$

Figure 3 compares the results from our current CFD simulations with the experimental data from Salta and Kröger [22] and the numerical findings reported by Duvenhage et al. [23].

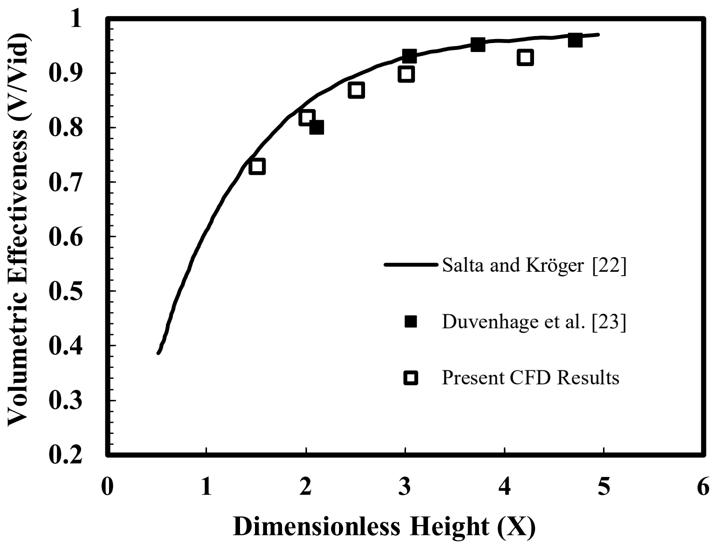

Figure 3 Validation of the present results with the experimental data by Salta and Kröger [22] and numerical results by Duvenhage et al. [23]

It is important to note that this validation approach has also been utilized by Meyer [24] and Bredell et al. [25] in their respective studies. Table 3 presents the geometrical details of the cases used for this comparison.

The results shown in Figure 3 indicate that the variations in volumetric effectiveness predicted by our simulations are in reasonable agreement with the experimental and numerical results from previous studies. This suggests that our developed model is both robust and reliable.

Table 3 Geometrical parameters of the cases in other investigations compared to the present study

Research	W_F/d_F	n_{FR}	d_H/d_F
Salta and Kröger [21]	1.27	2, 4, 8, 12	0.26
Duvenhage et al. [22]	1.18	2	0.232
Meyer [23]	1.27	2, 4	0.4
Bredell et al. [24]	1.29	6	0.153
Present research	1.66	7	0.25

5. Results and discussion

To analyze the performance of the heat collector for a large-scale ASHP, we should examine the temperature ratio at the inlet and outlet of the fans, taking the ambient temperature into account. To achieve this, we have defined a mathematical relationship between these temperatures. In heat collector of large-scale ASHP, higher temperatures at the fan inlets are associated with lower recirculation rates, indicating better performance of the device. Equation (5) outlines the parameters used to analyze the performance of the heat collector of the large-scale ASHP. This definition shows that the recirculation rate (*RR*) varies with the temperatures at the fans' inlets and outlets. Typically, this parameter is based on the average temperature values for all the fans. According to this equation, higher inlet temperatures for the fans result in lower *RR* values, which demonstrates improved performance. In our analysis, the ambient temperature is assumed to be 10 *°C*.

$$Recirculation\ Rate\ (RR)=(T_{in}-T_{amb})/(T_{out}-T_{amb}) \tag{5}$$

To test the performance of the simulated heat collector under different scenarios, we defined cases based on varying wind speeds, specifically Case a to Case d. These cases were designed to evaluate the impact of wind speed on the performance of the units, measured as the recirculation rate (*RR*). Table 4 presents the average results for the inlet temperature of the fans (T_{in}), the outlet temperatures of the fans (T_{out}), and the corresponding average values for *RR* in each case.

The results indicate that as the wind speed increases from 0 *m/s* to 5 *m/s*, both the inlet and outlet temperatures of the fans decrease. Since the outlet temperature is related to the inlet temperature as described in Equation (1), a decrease in the inlet temperature leads to a decrease in the outlet temperature. Consequently, the value of *RR* increases with the wind velocity, indicating that the performance of the units decreases with rising wind speeds. However, when the wind speed increases further from 5 *m/s* to 8 *m/s*, the performance of the unit improves. Therefore, we can conclude that wind velocity does not necessarily decrease the units' performance. There is a specific wind speed range; as the wind speed increases from 0 to this particular value, the performance decreases, but beyond this point, increasing wind speed enhances the efficiency of the heat collector.

Table 4 Average temperature values for the simulated models

	Wind Speed (*m/s*)	T_{in} (°C)	T_{out} (°C)	*RR*
Case a	0	9.95	3.97	0.007
Case b	2	9.30	3.71	0.108
Case c	5	8.67	3.46	0.188
Case d	8	8.93	3.57	0.145

This performance pattern should be further investigated by taking into account other thermophysical properties to create a logical foundation for justifying these phenomena. To illustrate this, Figure 4 shows the affected area resulting from the cold air produced by the heat collector of the large-scale ASHP, presented from a top-down view and considering different wind velocities. As observed in Figure 4, the upstream affected distance in the no-wind scenario (Case a) is the largest, measuring 300 *m*. This distance significantly decreases as wind velocity increases.

A notable trend illustrated in the figure is that the impact of the cold air on the surrounding area is diminished by higher wind speeds. The significance of the contours and results in Figure 4 becomes especially important when considering the placement of heat collector near buildings or other facilities. Therefore, it is essential to account for the effect of the cold air produced and the extent of its influence on nearby buildings and structures.

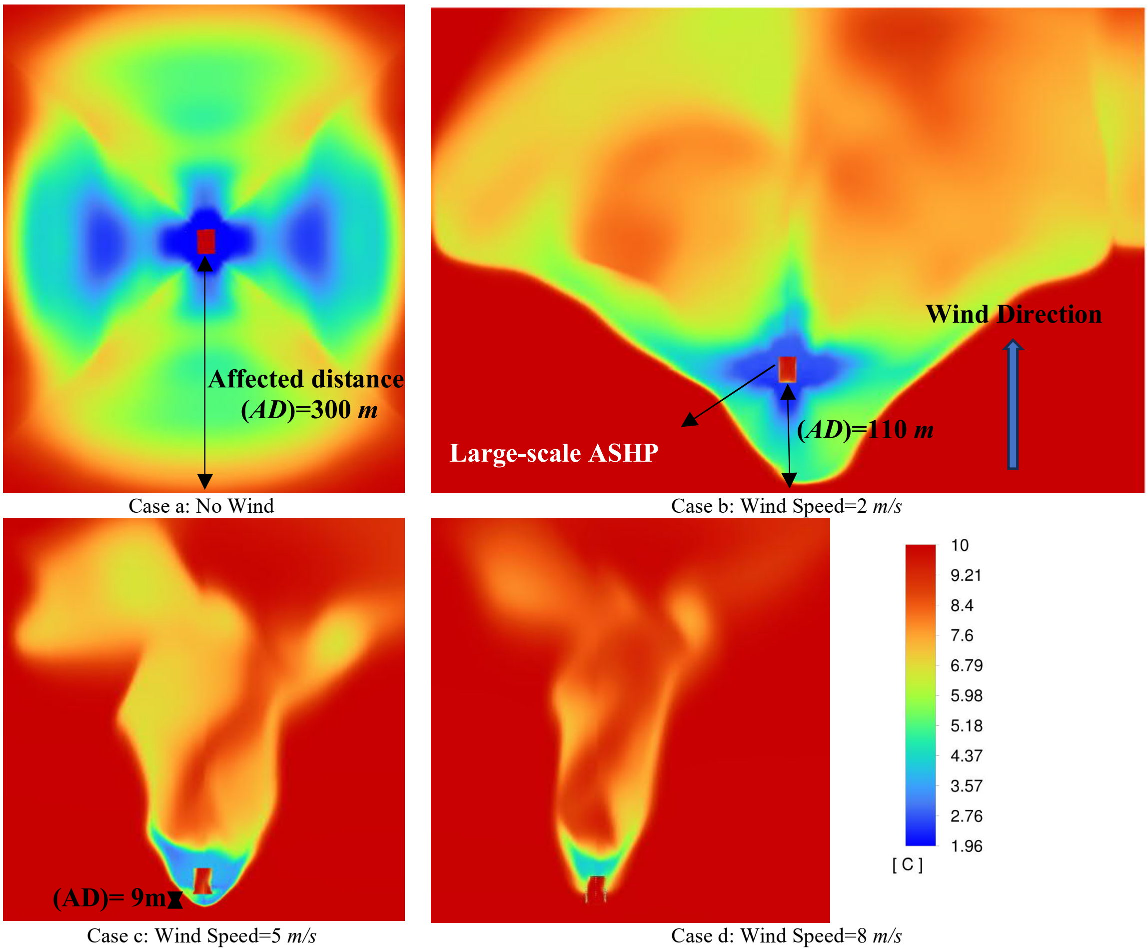

Figure 4 Temperature field for the simulated heat collector of the large-scale air source heat pump from up view at ground level (height=0 *m*)

To gain a clear understanding of the performance phenomena associated with the heat collector, it is essential to closely analyze the units and examine the temperature patterns at the fan inlets, which are influenced by the surrounding flow field. Figure 5 provides a close-up view of these units, illustrating the temperature changes at the fan inlets. It is important to note that the color maps for Figures 4 to 7 are identical. In Case a, where there is no wind, the temperatures at the fan inlets are very close to the ambient temperature, resulting in the lowest *RR* and the highest performance, as confirmed by the data in Table 4. Figure 5 indicates that when wind velocity increases from 0 to 2 *m/s*, there are noticeable temperature variations in three zones: A2, A3, and A4. Specifically, the fans labeled 8*j*2 (where *j* ranges from 1 to 7) in Zone A2 (black dotted ellipse), fans *k*7*i* (where *k* ranges from 3 to 7 and *i* is 1 or 2) in Zone A4 (green dotted ellipse), and fans *k*1*i* (where *k* ranges from 3 to 7 and *i* is 1 or 2) in Zone A3 (yellow dotted ellipse) are affected by the wind flow patterns. As the wind velocity increases from 2 *m/s* to 5 *m/s*, the number of affected fans in Zone A2 significantly decreases. Conversely, the fans *k*7*i* (where *k* ranges from 3 to 7 and *i* is 1 or 2: green rectangle) in Zone A4 and fans *k*1*i* (where *k* ranges from 3 to 7 and *i* is 1 or 2: yellow rectangle) in Zone A3 experience increased impact compared to the previous scenario (when wind velocity was 2 *m/s*). Additionally, at a wind velocity of 5 *m/s*, some fans in A2 and A4 areas are influenced by the cold air generated by the heat collector and the wind flow field (blue rectangle).

When the wind velocity increased from 5 *m/s* to 8 *m/s*, there was a significant change in the temperature variation at the inlets of the fans. Comparing Cases c and d, the impact of the cold air on the fans in Zone A2 has nearly dissipated. In contrast, a stronger effect is observed in Zone A1. As shown in Figure 5, Fans 1*ji* (where *j*=6 and 7, and *i*=1 or 2: black dotted circle) in Zone A1 are significantly affected by the cold air circulation, while the effects in Zones A3 and A4 have decreased. From the observed patterns of temperature variation between Cases c and d, we can conclude that the decreasing effects are stronger than the increasing effects. Therefore, we anticipate that the *RR* value will decrease from Case c to Case d, which aligns well with the results presented in Table 4. Additionally, it is worth noting that the fans and their performance are surprisingly good. The areas most affected by the cold air circulation are located close to the fans' intakes, indicating that the fans' suction is operating effectively (black ellipses).

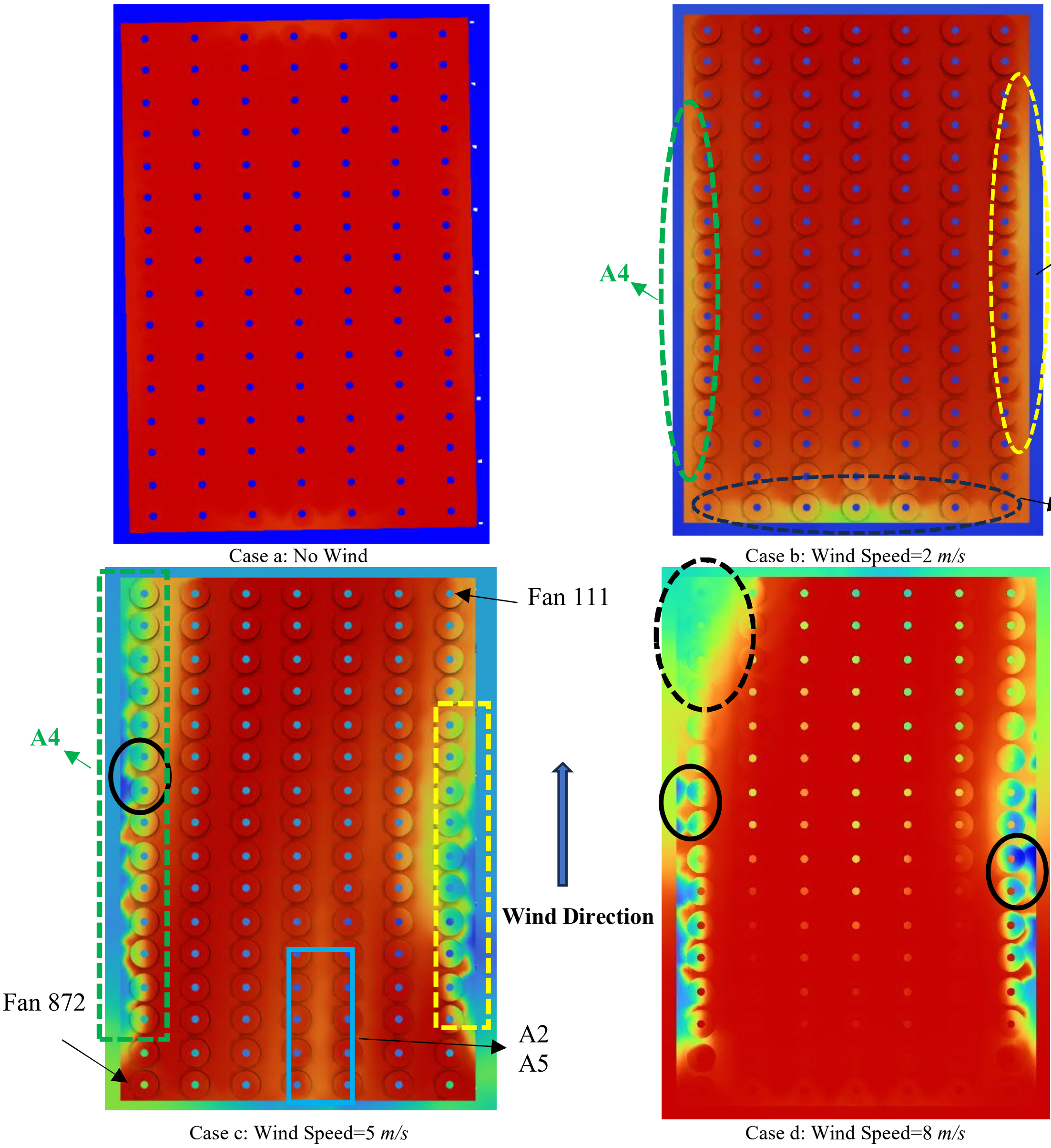

Figure 5 Variation of the temperature at the fans' inlets considering different wind velocities.

To understand the phenomena related to the temperature variations in the units at different wind speeds (see Figure 5), it is crucial to examine the fluid flow around the heat collector. For this reason, Figure 6 illustrates the flow streamlines in the x-direction, which represents the wind direction. In Case a, where there is no wind, no circulation is detected. Figure 6 presents the cases with wind velocity. At a wind speed of 2 *m/s*, there is a significant vortex formed in front of the units (upstream), which enhances the circulation of the cold air produced by the units toward the fan inlets. The area most affected by this vortex is Zone A2. From the streamlines shown in Figure 6, it is expected that the fan inlets in Zone A2 have lower temperatures compared to those farther away. This observation is fully supported by Figure 5. We can conclude that the presence of circulation around the units is a critical factor in determining the performance of a heat collector. Additionally, the prominent vortex indicates the areas influenced by cold air circulation, as seen in Figure 4. Figure 6 demonstrates that as the wind velocity increases from 2 m/s to 5 m/s, the size of the vortex in front of the units diminishes. This decreasing trend is clearly reflected in the affected area shown in Figure 4. When the wind velocity reaches 8 *m/s*, the vortex nearly disappears, which significantly reduces the impact of the cold air produced by the units on the fan inlets, especially in Zone A2. Consequently, the affected area by the cold circulation in this scenario (Zone A2) is minimal compared to the other cases, as confirmed by Figure 4. Overall, the flow field analysis in the x-direction is a key factor in understanding how a heat collector of large-scale ASHP interacts with ambient conditions, particularly in zones like A2.

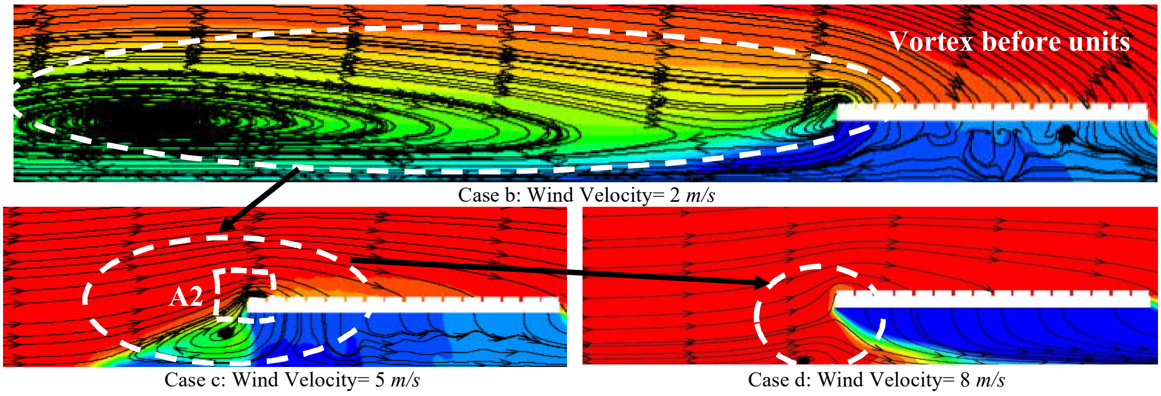

Figure 6 Streamlines and flow patterns in x direction for different wind velocities (with temperature contours in background)

Figure 7 illustrates the streamline patterns in the f4 direction with temperature contours under different wind velocities. The vortices surrounding the units have been labeled according to their respective cases. As depicted in Figure 7, two vortices appear on both sides of the units across all cases. These vortices influence the fans in Zones A3 and A4. The streamline patterns clearly demonstrate how the cold air generated by the units affects the temperature at the associated fans. As the wind velocity increases from 2 *m/s* to 5 *m/s*, the b1 and b2 vortices become stronger and transform into c1 and c2. The presence of these stronger vortices around the units leads to an increase in *RR* and a decrease in the performance of the heat collector. This relationship is also clearly presented in Table 4 and is observable in Figure 5. When the wind velocity increases from 5 *m/s* to 8 *m/s*, the sizes of the c1 and c2 vortices diminish, transforming into d1 and d2 vortices. Therefore, it is expected that this decreasing trend in vortex size from Case c to Case d will result in an improvement in the performance of the heat collector, as confirmed by the data presented in Table 4. In conclusion, all phenomena related to flow behavior around the units directly affect the performance of the device. The model presented in this study effectively illustrates and justifies the relationship between these phenomena and variations in performance.

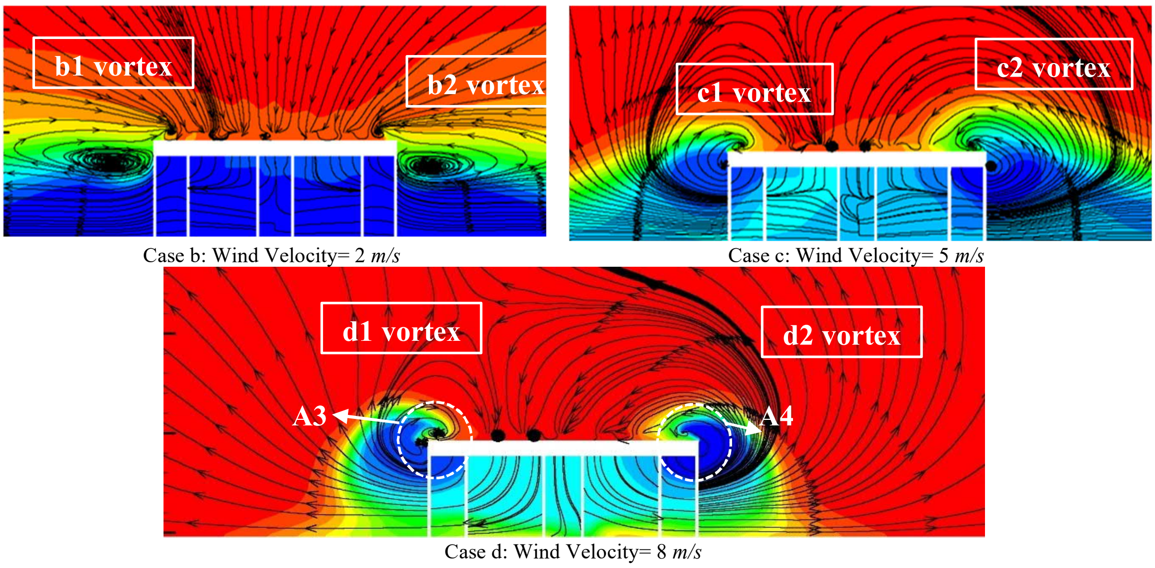

Figure 7 Streamlines and flow patterns in f4 direction for different wind velocities (with temperature contours in background)

6. Conclusions

This research introduces an innovative and precise 3D-CFD model designed to predict the performance of heat collector of large-scale air-source heat pumps (ASHP). This new approach allows each fan to operate independently, meaning the mass flow rate is not fixed. As the temperature changes, so does the density of the air at the fan inlets. This model establishes a strong connection between the flow phenomena surrounding the units and the resulting performance variations. The model has been tested under various wind velocities, leading to the following key conclusions:

1. As wind velocity increases from 0 *m/s*, the performance of the heat collector initially decreases. However, when the wind velocity exceeds 5 *m/s*, the performance begins to increase.
2. Increasing wind velocity reduces the size of the vortex formed upstream of the units.
3. Larger vortices near the units negatively impact the performance of the heat collector.
4. The upstream affected area by the airflow around the heat collector diminishes as wind velocity increases.
5. Examining the area affected by the cold air produced by the units in various environmental conditions is essential for constructing other facilities or buildings around heat collectors.

The presented interactive model demonstrates strong correlation with experimental data from other researchers, indicating its good reliability.

Suggestions for future studies:

1) Using the k-Omega SST turbulence model to detect more accurate vortex shapes regarding the domain of the heat collector.
2) Analyzing the effect of different wind directions on the performance of the heat collector.

References

[1] I. P. o. C. C. (IPCC), "Sixth assessment report: Climate change," vol. https://www.ipcc.ch/report/ar6/wg1/, 2021.

[2] X. Meng, X. Zhou and Z. Li, "Review of the Coupled System of Solar and Air Source Heat Pump," Energies , vol. 17, no. 23, 2024.

[3] G. Yeqing and L. Hua, "Research on China's Total Energy Consumption and Energy Structure," Mediterranean Journal of Social Sciences, vol. 4, no. 9, 2013.

[4] W. Zhao, B. Zhu, S. J. Davis, P. Ciais, C. Hong, Z. Liu and P. Gentine, "Reliance on fossil fuels increases during extreme temperature events in the continental United States," Communications Earth & Environment, vol. 4, 2023.

[5] Y. Ren, "Comprehensive Evaluation of Three Major Heat Pump Technologies: Air-Source, Ground-Source, and Water-Source Heat Pump," Applied and Computational Engineering, vol. Proceedings of the 3rd International Conference on Functional Materials and Civil Engineering, 2025.

[6] D. Romanov and B. Leiss, "Geothermal energy at different depths for district heating and cooling of existing and future building stock," Renewable and Sustainable Energy Reviews, vol. 167, 2022.

[7] F. Alshehri, S. Beck, D. Ingham, L. Ma and M. Pourkashanian, "Techno-economic analysis of ground and air source heat pumps in hot dry climates," Journal of Building Engineering, vol. 26, 2019.

[8] D. Jenkins, R. Tucker, M. Ahadzi and R. Rawlings, "The performance of air-source heat pumps in current and future offices," Energy and Buildings, vol. 40, no. 10, 2008.

[9] U. Berardi and S. Jones, "The efficiency and GHG emissions of air source heat pumps under future climate scenarios across Canada," Energy and Buildings, vol. 262, 2022.

[10] P. M. Congedo, C. Baglivo, D. D'Agostino and D. Mazzeo, "The impact of climate change on air source heat pumps," Energy Conversion and Management, vol. 276, 2023.

[11] K. Sezen and A. Gungor, "Performance analysis of air source heat pump according to outside temperature and relative humidity with mathematical modeling," Energy Conversion and Management, vol. 263, 2022.

[12] W. Kim and J. E. Braun, "Evaluation of the impacts of refrigerant charge on air conditioner and heat pump performance," International Journal of Refrigeration, vol. 35, no. 7, 2012.

[13] A. R. Jafri, "Experimental Investigation of Building Envelope and Air Source Heat Pumps in Canadian Cold Climate," A thesis:School of Graduate and Postdoctoral Studies, vol. University of Ontario Institute of Technology (Ontario Tech University).

[14] M. Liu, X. Xie, W. Yang, F. Xu, S. Gao, L. Ding and H. Liang, "A two-level optimal scheduling control strategy for air source heat pump loads with phase change energy storage," IET Generation, Transmission & Distribution, vol. 19, no. 1, 2024.

[15] K. Sezen, A. D. Tuncer, A. O. Akyuz and A. Gungor, "Effects of ambient conditions on solar assisted heat pump systems: a review," Science of The Total Environment, vol. 778, 2021.

[16] X.-M. Guo, Y.-G. Chen, W.-H. Wang and C.-Z. Chen, "Experimental study on frost growth and dynamic performance of air source heat pump system," Applied Thermal Engineering, vol. 28, 2008.

[17] S. Wang, W. Wei, W. Wang, Y. Sun, Z. Li, C. Dai, C. Huang, R. Tang and S. Deng, "Frosting-defrosting performance variations of air source heat pumps with the type of refrigerants: R410A and R32 as an example," Applied Thermal Engineering, vol. 262, 2025.

[18] J. Nie, K. Wang, X. Kong, H. Zhang and S. Zhang, " Theoretical Study and Experimental Validation on the Applicable Refrigerant for Space Heating Air Source Heat Pump," Sustainability , vol. 15, no. 12, 2023.

[19] J. Heo, M. W. Jeong, C. Baek and Y. Kim, "Comparison of the heating performance of air-source heat pumps using various types of refrigerant injection," International Journal of Refrigeration, vol. 34, no. 2, 2011.

[20] B. Rogié, J. K. Jensen, S. O. K. Hansen and W. B. Markussen, "Analysis of Cold Air Recirculation in the Evaporators of Large-Scale Air-Source Heat Pumps Using CFD Simulations," Fluids , vol. 5, no. 4, 2020.

[21] ANSYS, Inc. (2021). ANSYS Fluent, Release 21R2.

[22] C. Salta and D. Kro¨ger, "Effect of inlet flow distortions on fan performance in forced draft air-cooled heat exchangers," Heat Recovery Systems & CHP, p. 555–561, 1995.

[23] K. Duvenhage, J. Vermeulen, C. Meyer and D. Kro¨ger, "Flow distortions at the fan inlet of forced draft air-cooled heat exchangers," Applied Thermal Engineering, vol. 16, p. 741–752, 1996.

[24] C. Meyer, "Numerical investigation of the effect of inlet flow distortions on forced draft air-cooled heat exchanger performance," Applied Thermal Engineering, vol. 25, p. 1634–1649, 2005.

[25] J. Bredell, D. G. Kröger and G. D. Thiart, "Numerical investigation of fan performance in a forced draft air-cooled steam condenser," Applied Thermal Engineering, vol. 26, no. 8, pp. 846-852, 2006.